

Probing Lepton Asymmetry with 21 cm Fluctuations

Kazunori Kohri^{1,2}, Yoshihiko Oyama¹, Toyokazu Sekiguchi^{3,4}
and Tomo Takahashi⁵

¹ *The Graduate University for Advanced Studies (Sokendai), 1-1 Oho, Tsukuba
305-0801, Japan*

² *Institute of Particle and Nuclear Studies, KEK, 1-1 Oho, Tsukuba 305-0801, Japan*

³ *Graduate School of Science, Nagoya University, Furo-cho, Chikusa-ku, Nagoya,
464-8602, Japan*

⁴ *Helsinki Institute of Physics, University of Helsinki, PO Box 64, FIN-00014*

⁵ *Department of Physics, Saga University, Saga 840-8502, Japan*

Abstract

We investigate the issue of how accurately we can constrain the lepton number asymmetry $\xi_\nu = \mu_\nu/T_\nu$ in the Universe by using future observations of 21 cm line fluctuations and cosmic microwave background (CMB). We find that combinations of the 21 cm line and the CMB observations can constrain the lepton asymmetry better than big-bang nucleosynthesis (BBN). Additionally, we also discuss constraints on ξ_ν in the presence of some extra radiation, and show that the 21 cm line observations can substantially improve the constraints obtained by CMB alone, and allow us to distinguish the effects of the lepton asymmetry from the ones of extra radiation.

1 Introduction

The issue of the asymmetry of matter and antimatter in the Universe is one of the important subject in cosmology and particle physics. The baryon asymmetry is now accurately determined by using the combination of cosmological observations such as cosmic microwave background (CMB), big bang nucleosynthesis (BBN), large scale structure, type Ia supernovae and so on, and its actual number is $\eta = (n_b - n_{\bar{b}})/n_\gamma \simeq 6 \times 10^{-10}$ with $n_b, n_{\bar{b}}$ and n_γ being the number densities of baryon, anti-baryon and photon, respectively. However, on the other hand, the asymmetry in the leptonic sector, the lepton asymmetry, is not well measured and only a weak constraint for the neutrino degeneracy parameter $\xi_\nu = \mu_\nu/T_\nu$ is obtained^{#1}. Although the lepton asymmetry is expected to be the same order with the baryonic one due to the spharelon effect, in some models, it can be much larger than the baryonic one [6–10]. Furthermore, if the lepton asymmetry is large, it may significantly affect some aspects of the evolution of the Universe: QCD phase transition [11], large-scale cosmological magnetic field [12], density fluctuations if primordial fluctuation is generated via the curvaton mechanism [13–15] and so on.

Thus it would be worth investigating to what extent the lepton asymmetry can be probed beyond the accuracy of current cosmological observations. Although various cosmological surveys are planned in the future, we in this paper consider future observations of fluctuations of neutral hydrogen 21 cm line, in addition to those of CMB, to study the future prospects of measuring the lepton asymmetry in the Universe. Since the signals from the 21 cm line can cover a wide redshift range, they can be complementary to other observations such as CMB. In addition, the effects of the lepton asymmetry mainly appear on small scales, which can be well measured by 21 cm observations. Thus such a survey would provide useful information. In this paper, to discuss expected constraints from the future cosmological surveys on the lepton asymmetry, or more specifically, the degeneracy parameter ξ_ν , we make Fisher analysis by assuming the specifications for planned observations of 21 cm fluctuations such as Square Kilometer Array (SKA) [16] and Omniscience [17]. We also take into account BBN and CMB observations such as Planck [18] and CMBPol [19].

The structure of this paper is as follows. In the next section, we summarize the formulas to investigate the effects of the lepton asymmetry on CMB and 21 cm fluctuations. Then in Section 3, we present our results, paying particular attention to how 21 cm observations will help to probe the lepton asymmetry. Summary and conclusion of this paper is given in the final section.

^{#1} So far constraints on ξ_ν have been obtained by BBN (e.g., see [1, 2] and Fig. 4 in Appendix C), which is sometimes combined with CMB and/or some other observations (e.g., see Refs. [3–5]).

2 Lepton asymmetry

In this section, we summarize the formulas to calculate power spectra of CMB and 21 cm fluctuations in models with non-zero lepton asymmetry, or non-zero chemical potential for neutrinos. When there exist nonzero chemical potentials for neutrinos, they affect its energy density and pressure, which modifies the background evolution. The existence of non-zero chemical potential also alters the perturbation equation. Below we describe the changes of the background and perturbation parts in turn.

2.1 Background

The distribution function for neutrino species ν_i and its anti-particle $\bar{\nu}_i$ with $i = e, \mu, \tau$ are given by

$$f_{\nu_i}(p_i) = \frac{1}{e^{p_i/T_\nu + \xi_{\nu_i}} + 1}, \quad f_{\bar{\nu}_i}(p_i) = \frac{1}{e^{p_i/T_\nu - \xi_{\nu_i}} + 1}, \quad (1)$$

where p_i is momentum of ν_i . ξ_{ν_i} is the degeneracy parameter which is defined as $\xi_{\nu_i} \equiv \mu_{\nu_i}/T_\nu$ with μ_{ν_i} being the chemical potential for ν_i . T_ν is the temperature of neutrino and related to that at the present epoch T_{ν_0} as $T_\nu = T_{\nu_0}/a$ with a being the scale factor.

In the following, we omit the subscript i for simplicity and give the formulas for one neutrino species including its mass m . The effects of the lepton asymmetry on the background evolution appear as the changes in its energy density and pressure. The energy density and pressure of a neutrino species are given by

$$\rho_\nu + \rho_{\bar{\nu}} = \frac{1}{2\pi^2} \int_0^\infty p^2 dp \sqrt{p^2 + m^2} (f_\nu + f_{\bar{\nu}}), \quad (2)$$

$$p_\nu + p_{\bar{\nu}} = \frac{1}{2\pi^2} \int_0^\infty p^2 dp \frac{p^2}{3\sqrt{p^2 + m^2}} (f_\nu + f_{\bar{\nu}}). \quad (3)$$

By using the comoving momentum $q \equiv pa$, the above integral can be rewritten as

$$\rho_\nu + \rho_{\bar{\nu}} = \frac{T_\nu^4}{2\pi^2} \int_0^\infty y^3 dy \sqrt{1 + \left(\frac{a\tilde{m}}{y}\right)^2} \left(\frac{1}{e^{y+\xi} + 1} + \frac{1}{e^{y-\xi} + 1} \right), \quad (4)$$

$$p_\nu + p_{\bar{\nu}} = \frac{T_\nu^4}{6\pi^2} \int_0^\infty y^3 dy \frac{1}{\sqrt{1 + (a\tilde{m}/y)^2}} \left(\frac{1}{e^{y+\xi} + 1} + \frac{1}{e^{y-\xi} + 1} \right), \quad (5)$$

where we have defined y and \tilde{m} as

$$y \equiv \frac{q}{T_{\nu_0}}, \quad \tilde{m} \equiv \frac{m}{T_{\nu_0}}. \quad (6)$$

Although in general, the above integrals should be performed numerically, in relativistic and non-relativistic limits, some useful approximation can be adopted, in particular, when $|\xi| \ll \mathcal{O}(1)$. Below we give explicit formulas for each case.

- **Relativistic limit**

When $\frac{a\tilde{m}}{y}(=\frac{m}{p}) \ll 1$, by expanding the integrand in Eqs. (2) and (3) up to the 2nd order in $\frac{a\tilde{m}}{y}$, the energy density and pressure can be written as

$$\rho_\nu + \rho_{\bar{\nu}} \simeq \frac{T_\nu^4}{2\pi^2} \int_0^\infty y^3 dy \left(1 + \frac{1}{2} \left(\frac{a\tilde{m}}{y} \right)^2 \right) \left(\frac{1}{e^{y+\xi} + 1} + \frac{1}{e^{y-\xi} + 1} \right), \quad (7)$$

$$p_\nu + p_{\bar{\nu}} \simeq \frac{T_\nu^4}{6\pi^2} \int_0^\infty y^3 dy \left(1 - \frac{1}{2} \left(\frac{a\tilde{m}}{y} \right)^2 \right) \left(\frac{1}{e^{y+\xi} + 1} + \frac{1}{e^{y-\xi} + 1} \right). \quad (8)$$

These integrals can be performed exactly and we obtain

$$\rho_\nu + \rho_{\bar{\nu}} \simeq \frac{7\pi^2}{120} T_\nu^4 \left[\left\{ 1 + \frac{30}{7} \left(\frac{\xi}{\pi} \right)^2 + \frac{15}{7} \left(\frac{\xi}{\pi} \right)^4 \right\} + \frac{5}{7\pi^2} (a\tilde{m})^2 \left\{ 1 + 3 \left(\frac{\xi}{\pi} \right)^2 \right\} \right], \quad (9)$$

$$p_\nu + p_{\bar{\nu}} \simeq \frac{1}{3} \frac{7\pi^2}{120} T_\nu^4 \left[\left\{ 1 + \frac{30}{7} \left(\frac{\xi}{\pi} \right)^2 + \frac{15}{7} \left(\frac{\xi}{\pi} \right)^4 \right\} - \frac{5}{7\pi^2} (a\tilde{m})^2 \left\{ 1 + 3 \left(\frac{\xi}{\pi} \right)^2 \right\} \right]. \quad (10)$$

- **Non-relativistic limit**

When $\frac{a\tilde{m}}{y}(=\frac{m}{p}) \gg 1$, we can expand Eq. (2) around $y/(a\tilde{m}) = 0$ and $\xi = 0$ ^{#2} as

$$\begin{aligned} \rho_\nu + \rho_{\bar{\nu}} &= \frac{T_\nu^4}{2\pi^2} \int_0^\infty y^3 dy \frac{a\tilde{m}}{y} \sqrt{\left(\frac{y}{a\tilde{m}} \right)^2 + 1} \left(\frac{1}{e^{y+\xi} + 1} + \frac{1}{e^{y-\xi} + 1} \right) \\ &\simeq \frac{T_\nu^4 a\tilde{m}}{2\pi^2} \int_0^\infty y^2 dy \left[1 + \frac{1}{2} \left(\frac{y}{a\tilde{m}} \right)^2 \right] \left(\frac{1}{e^{y+\xi} + 1} + \frac{1}{e^{y-\xi} + 1} \right) \\ &\simeq \frac{T_\nu^4 a\tilde{m}}{2\pi^2} \int_0^\infty y^2 dy \left[1 + \frac{1}{2} \left(\frac{y}{a\tilde{m}} \right)^2 \right] \sum_i C_i(y) \xi^i, \end{aligned} \quad (11)$$

where $C_i(y)$ are the coefficients for the expansion of $((e^{y+\xi} + 1)^{-1} + (e^{y-\xi} + 1)^{-1})$ around $\xi = 0$. We note that the terms with odd power for ξ do not appear. Explicit formulas for $C_i(y)$ are given in Appendix A.

Having the expressions for $C_i(y)$, we can analytically perform the integral of the form:

$$\int_0^\infty C_i(y) y^2 dy, \quad \text{and} \quad \int_0^\infty C_i(y) y^4 dy. \quad (12)$$

^{#2} In a non-relativistic limit for any ξ values, the exact solutions of $\rho_\nu + \rho_{\bar{\nu}}$ and $p_\nu + p_{\bar{\nu}}$ are expressed by using polylogarithm. The formulas are given in Appendix B.

By taking into account the terms up to the 10th order in ξ , we obtain

$$\begin{aligned} \rho_\nu + \rho_{\bar{\nu}} \simeq & \frac{T_\nu^4}{2\pi^2} (a\tilde{m}) \left[3\zeta(3) + (\log 4)\xi^2 + \frac{1}{24}\xi^4 - \frac{1}{1440}\xi^6 + \frac{1}{40320}\xi^8 - \frac{17}{14515200}\xi^{10} \right] \\ & + \frac{T_\nu^4}{4\pi^2} \frac{1}{a\tilde{m}} \left[45\zeta(5) + 18\zeta(3)\xi^2 + (\log 4)\xi^4 + \frac{1}{60}\xi^6 - \frac{1}{6720}\xi^8 + \frac{1}{302400}\xi^{10} \right], \end{aligned} \quad (13)$$

where $\zeta(x)$ means the Riemann zeta function. Similar calculations also hold for the pressure, and we have, up to the 10th order in ξ ,

$$\begin{aligned} p_\nu + p_{\bar{\nu}} \simeq & \frac{T_\nu^4}{6\pi^2} \frac{1}{a\tilde{m}} \left[45\zeta(5) + 18\zeta(3)\xi^2 + (\log 4)\xi^4 + \frac{1}{60}\xi^6 - \frac{1}{6720}\xi^8 + \frac{1}{302400}\xi^{10} \right] \\ & - \frac{T_\nu^4}{12\pi^2} \left(\frac{1}{a\tilde{m}} \right)^3 \left[\frac{2835\zeta(7)}{2} + 675\zeta(5)\xi^2 + 45\zeta(3)\xi^4 + (\log 4)\xi^6 + \frac{1}{112}\xi^8 - \frac{1}{20160}\xi^{10} \right]. \end{aligned} \quad (14)$$

We have checked that above formulas are accurate as 10^{-7} for $|\xi| < 1$ to obtain ρ_ν and p_ν with non-zero ξ .

2.2 Perturbation equation

Here we discuss the perturbation equation for massive neutrinos including the chemical potential. By perturbing the phase-space distribution function f_ν as [20]

$$\delta f_\nu(\tau, \vec{x}, \vec{p}) + \delta f_{\bar{\nu}}(\tau, \vec{x}, \vec{p}) = (\bar{f}_\nu(p) + \bar{f}_{\bar{\nu}}(p)) \Psi_\nu(\tau, \vec{x}, \vec{p}), \quad (15)$$

where \bar{f}_ν and $\bar{f}_{\bar{\nu}}$ are the background distribution functions, and Ψ_ν represents its perturbation. τ is the conformal time. The perturbed Boltzmann equation for Ψ_ν for the Fourier mode \vec{k} in the synchronous gauge is given by

$$\dot{\Psi}_\nu + i \frac{y}{\sqrt{y^2 + a^2 \tilde{m}^2}} (\vec{k} \cdot \hat{n}) \Psi_\nu + \frac{d \ln(\bar{f}_\nu + \bar{f}_{\bar{\nu}})}{d \ln y} \left[\dot{\eta}_T - \frac{1}{2} (\dot{h}_L + 6\dot{\eta}_T) (\vec{k} \cdot \hat{n})^2 \right] = 0, \quad (16)$$

where h_L and η_T are metric perturbations, and a dot represents the derivative with respect to the conformal time (we follow the notations in [20]). \hat{n} is the direction of the momentum \vec{p} . We expand Ψ_ν with the Legendre polynomial as

$$\Psi_\nu(\tau, \vec{k}, \vec{p}) = \sum_{l=0}^{\infty} (-i)^l (2l+1) \Psi_{\nu l}(\tau, \vec{k}, p) P_l(\hat{k} \cdot \hat{n}), \quad (17)$$

with \hat{k} being the direction of \vec{k} . The evolution equations for each multiple moment in the synchronous gauge take the form:

$$\dot{\Psi}_{\nu 0} = -\frac{yk}{\sqrt{y^2 + a^2\tilde{m}^2}}\Psi_{\nu 1} + \frac{1}{6}\dot{h}_L\frac{d\ln(\bar{f}_\nu + \bar{f}_{\bar{\nu}})}{d\ln y}, \quad (18)$$

$$\dot{\Psi}_{\nu 1} = \frac{yk}{3\sqrt{y^2 + a^2\tilde{m}^2}}(\Psi_{\nu 0} - 2\Psi_{\nu 2}), \quad (19)$$

$$\dot{\Psi}_{\nu 2} = \frac{yk}{5\sqrt{y^2 + a^2\tilde{m}^2}}(2\Psi_{\nu 1} - 3\Psi_{\nu 3}) - \left(\frac{1}{15}\dot{h}_L + \frac{2}{5}\dot{\eta}_T\right)\frac{d\ln(\bar{f}_\nu + \bar{f}_{\bar{\nu}})}{d\ln y}, \quad (20)$$

$$\dot{\Psi}_{\nu l} = \frac{yk}{(2l+1)\sqrt{y^2 + a^2\tilde{m}^2}}(l\Psi_{\nu(l-1)} - (l+1)\Psi_{\nu(l+1)}), \quad (\text{for } l \geq 3). \quad (21)$$

The dependence on the chemical potential appears in the factor $d\ln(\bar{f}_\nu + \bar{f}_{\bar{\nu}})/d\ln y$, which can be written as [21]

$$\frac{d\ln(\bar{f}_\nu + \bar{f}_{\bar{\nu}})}{d\ln y} = -\frac{y(1 + \cosh \xi \cosh y)}{(\cosh \xi + \exp(-y))(\cosh \xi + \cosh y)}. \quad (22)$$

By making the modifications given above as well as those for the background quantities to CAMB [22], we calculate power spectra of CMB and 21 cm fluctuations and make a Fisher matrix analysis, whose results will be discussed in the next section.

3 Results

Now in this section, we discuss future prospects of the determination of the lepton asymmetry, or the chemical potentials for neutrino. For this purpose, we study expected constraints on ξ by making Fisher analysis adopting future observations of 21 cm fluctuations and CMB. In the analysis, we assume the specifications of SKA [16] and Omniscope [17] for 21 cm fluctuations and Planck [18]^{#3} and CMBPol [19] for CMB. Our methodology in the following analysis is basically the same as our previous one [27], thus we refer the readers to [27] for the details.

In the following analysis, we explore the parameter space which includes the degenerate parameter $\xi = \xi_{\nu_e} = \xi_{\nu_\mu} = \xi_{\nu_\tau}$ assuming the universal lepton asymmetry^{#4} and neutrino mass m_ν as well as the six standard cosmological parameters $(\Omega_\Lambda, \Omega_b h^2, \Omega_m h^2, \tau_{\text{reion}}, A_s, n_s)$ ^{#5}.

^{#3} Although the temperature data from Planck is already available, here we are going to combine CMB data with future 21cm observations, and hence we also treat Planck in the same manner as other future observations.

^{#4} Regardless of the initial value of $\xi_{\nu i}$ (with $i = e, \mu, \tau$) at the decoupling, the lepton asymmetry would be universal, due to the large mixing in neutrino mass matrix [28].

^{#5} Here Ω_Λ , Ω_b and Ω_m are respectively energy densities of the cosmological constant, baryon and matter, h is the Hubble parameter normalized as $H_0 = 100h$ km/s/Mpc, τ_{reion} is the optical depth for reionization, A_s and n_s are respectively the amplitude and the spectral index for the primordial power spectrum.

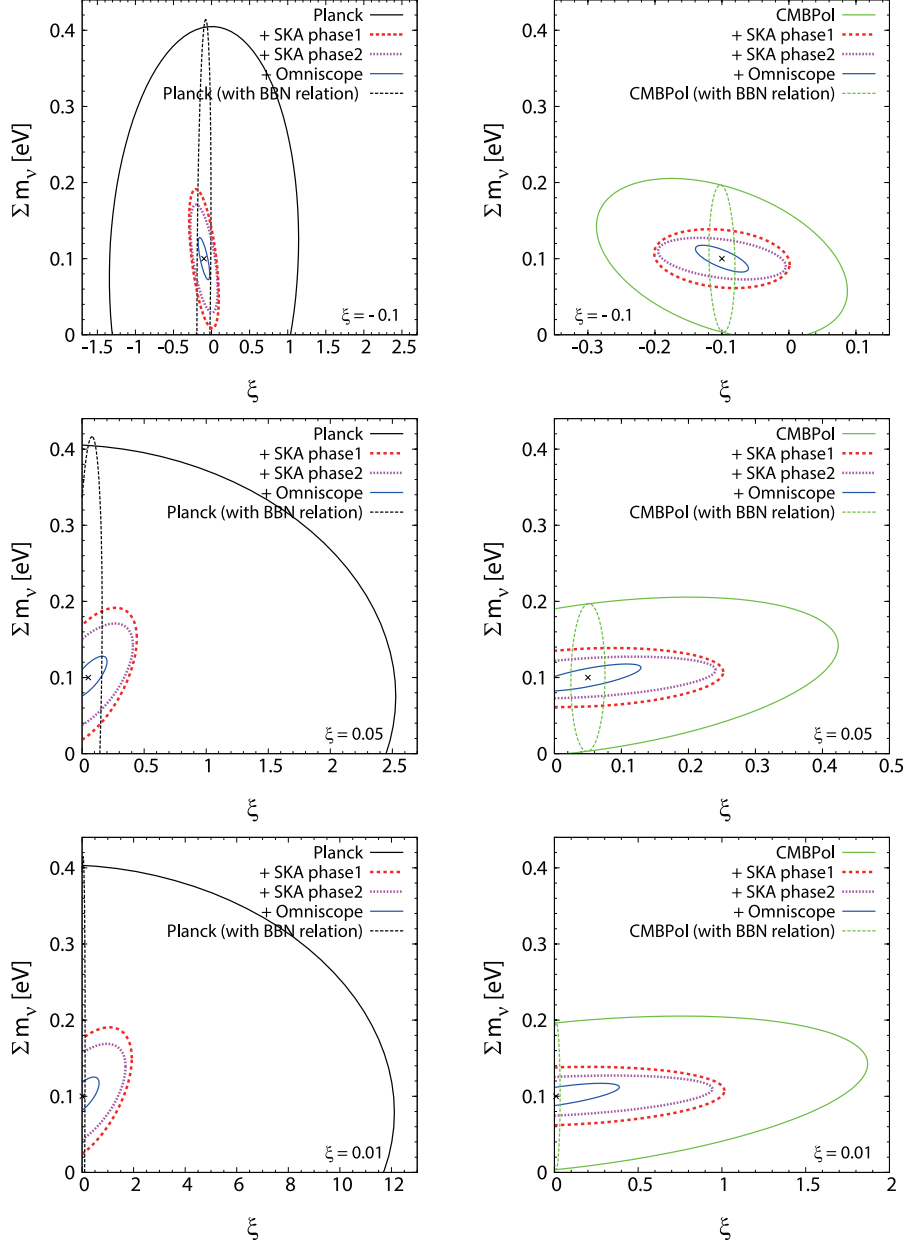


Figure 1: Expected 2σ constraints on the $\sum m_\nu$ - ξ plane. As CMB data, the Planck and CMBPol surveys are adopted in the left and right panels, respectively. In order from top to bottom, the fiducial values of ξ are set to -0.1 , 0.05 and 0.01 . Here we mainly present constraints for fixed $Y_p = 0.25$. Shown are the constraints from CMB alone (solid black/green line) as well as the ones from CMB data combined with 21 cm data from SKA phase1 (red line), SKA phase2 (magenta line) and Omniscope (blue line). As a reference, the constraints from CMB data alone with the BBN relation are also shown (dotted black/green line). Note that scales in x -axis differ among different panels.

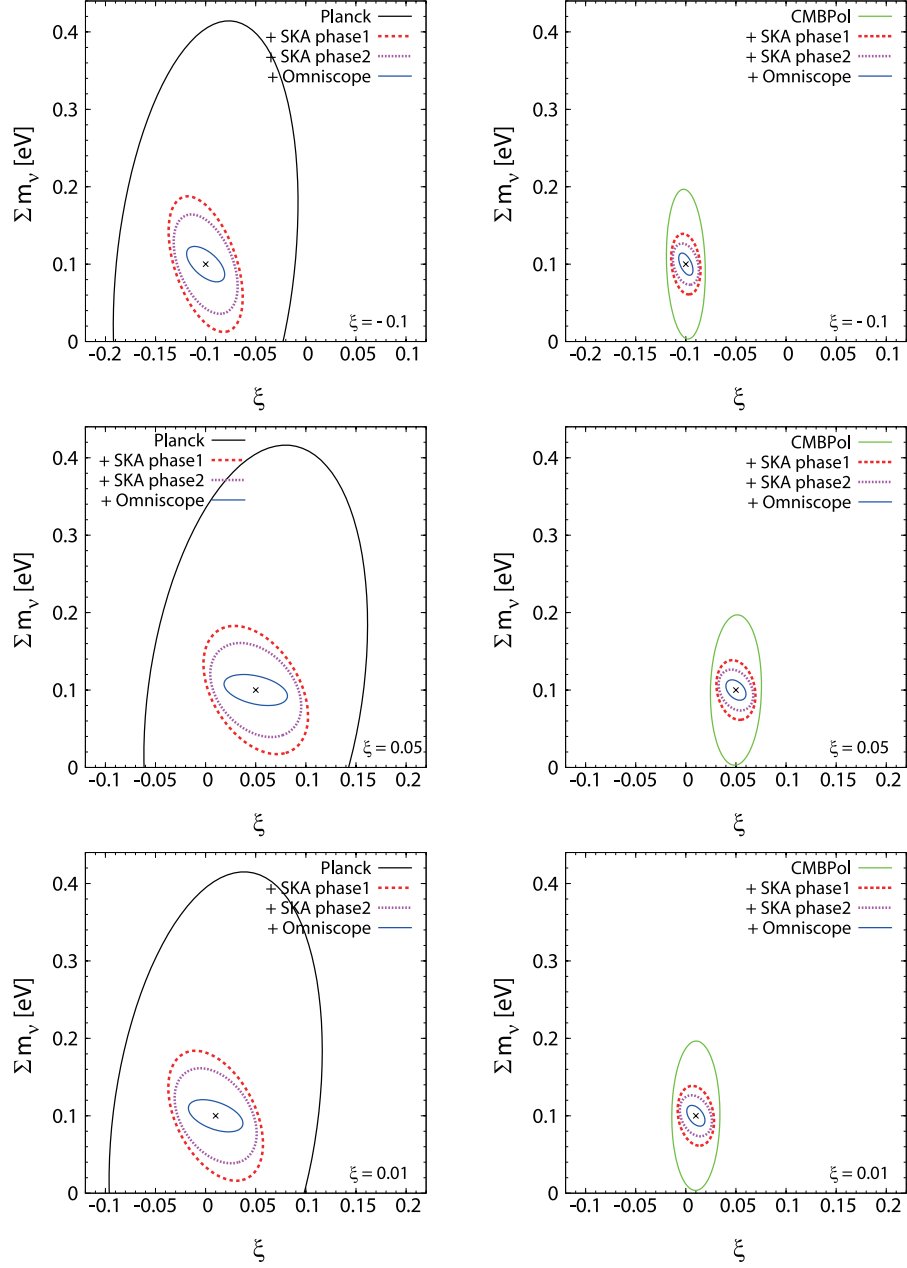


Figure 2: Expected 2σ constraints on the $\sum m_\nu$ - ξ plane. In this figure, the BBN relation is assumed.

In addition to these parameters, in some cases, we also include the helium abundance Y_p and the effective number of neutrino species for extra (dark) radiation ΔN_ν which gives its energy density in units of a single massless neutrino species as

$$\bar{\rho}_{\text{ext}} = \Delta N_\nu \frac{7\pi^2}{120} T_\nu^4. \quad (23)$$

Although the chemical potential ξ can be regarded as the changes to N_ν , that is, the effective number of neutrino species for total dark radiation (neutrinos and extra radiation) as seen from Eqs. (9) and (13), ΔN_ν counts for possible other contribution to N_ν . Furthermore, in BBN theory, Y_p is related to $\Omega_b h^2$, ξ and ΔN_ν . Therefore we make the analysis with/without assuming so-called BBN relation among these parameters in some analysis. When the BBN relation is not adopted, we vary Y_p freely or fix it to $Y_p = 0.25$.

Regarding fiducial parameters, we often present constraints for several fiducial values of ξ and ΔN_ν . On the other hand, fiducial values of $\sum m_\nu$ is fixed to be 0.1 eV and those of other cosmological parameters are fixed to be $(\Omega_\Lambda, \Omega_b h^2, \Omega_m h^2, \tau_{\text{reion}}, A_s, n_s) = (0.6914, 0.02216, 0.1417, 0.0952, 2.214 \times 10^{-9}, 0.9611)$, which are the best fit values from the Planck result [29].

3.1 Cases without extra radiation

Let us first see the cases without extra radiation. Fig. 1 shows constraints on the ξ - $\sum m_\nu$ plane for mainly the cases where we fixed Y_p to 0.25 without assuming the BBN relation. On the other hand, constraints only from CMB observations with the BBN relation $Y_p(\Omega_b h^2, \xi, \Delta N_\nu)$ are also shown as well, for the purpose of comparison. Regarding fiducial values of ξ , we adopted $\xi = 0.01, 0.05$ and -0.1 here. Note that $\xi = 0.05$ and -0.1 roughly correspond to the upper and lower bounds at 2σ from primordial abundance of the light elements (See Fig. 4 in Appendix C and Ref. [30]). From the figure, we can immediately see that 21 cm observations can be a powerful probes of the lepton asymmetry. Compared with the constraints on ξ from Planck alone, the error is improved by a factor around 5 (10) by combining SKA (Omniscope). Even though CMBPol can by itself give much tighter constraints than Planck, combinations with 21 cm observations are still able to improve the constraints further by a factor around 2 (SKA) and 4 (Omniscope). We also note that constraints on the neutrino masses from CMB observations can be also improved by combining 21 cm observations. As an illustrative example, constraints on cosmological parameters for the cases with fiducial $\xi = 0.05$ are summarized in Table 1.

In Fig. 1, one may notice that the uncertainties in ξ , which we denote as σ_ξ , is dependent on the fiducial value of ξ . This is because, in the absence of the BBN relation, there is no difference between neutrinos and anti-neutrinos in their effects both on the CMB and 21 cm power spectra. Therefore these power spectra are even functions of ξ , as can be also read from Eqs. (4)-(5) and (22), which respectively govern effects on the background and perturbation evolutions. In particular for small $\xi \ll 1$, these power spectra should respond linearly to ξ^2 . This leads that σ_ξ is proportional to the inverse of the fiducial ξ ,

while the error $\sigma_{\xi^2} \propto \xi \sigma_\xi$ is almost independent of the fiducial ξ , which is confirmed from Table 4, where we summarized constraints on ξ for various setups (e.g. without the BBN relation) and fiducial values of ξ for cases of $\Delta N_\nu = 0$.

Although σ_ξ is dependent on fiducial ξ , we can still see that $\xi = -0.1$, which is roughly the current lower bound from the primordial light elements, can be detected marginally by CMBPol+SKA and significantly by CMBPol+Omniscope. This is remarkable as this indicates that even without assuming the BBN relation, we may be able to obtain a constraint on ξ better than one from the primordial light elements.

On the other hand, from the above figure, one may think 21 cm alone is powerful enough to give similar constraints on ξ as those from CMB+21 cm. However, this is not true. This can be understood by seeing that provided a very precise observation of 21 cm, e.g., Omniscope, its combinations with Planck and CMBPol still differ non-negligibly. This is due to that some cosmological parameters which degenerate with ξ when only a 21 cm observation is adopted can be determined well by CMB.

Let us next see the cases with the BBN relation $Y_p(\Omega_b h^2, \xi, \Delta N_\nu)$, though we here still assume ΔN_ν to vanish. In this case, ξ affects CMB and 21 cm observations also through Y_p in addition to the effects we have taken into account in the case of fixed Y_p . Regarding effects of ξ on the CMB power spectrum, this indirect effect through the BBN relation is more significant than direct ones. This can be noticed in Fig. 1, where the contours of constraints from CMB alone can be squeezed in the direction of ξ by an order of magnitude with the BBN relation.

Fig. 2 shows the same constraints as in Fig. 1 except that the BBN relation is now taken into account in any combinations of observations. Compared with the previous figure, improvements brought about by the combination of 21 cm observations are not as dramatic as in the cases without the BBN relation. This indirectly suggests that 21cm observations are not as sensitive to Y_p as CMB. However, the combination with SKA can reduce the size of error in ξ by a few times from Planck alone and a similar level of improvement can be brought about by Omniscope compared to CMBPol alone. We note that with the BBN relation being assumed, a combination of CMB and 21 cm observations can constrain the lepton asymmetry substantially better than the primordial abundances of light elements.

Different from the cases without the BBN relation, one can notice that the sizes of errors in ξ little depend on fiducial ξ with the BBN relation. This is because prediction of BBN is sensitive to the sign of ξ . Therefore Y_p responses linearly to ξ at the lowest order. In particular, the most significant effect of ξ on Y_p is that ξ_e changes the ratio of neutron number density to proton one when BBN starts. Positive (negative) ξ effectively boosts (suppresses) $n \rightarrow p$ conversion and reduces (increases) Y_p . Such an effect can break the degeneracy between ξ and $-\xi$ existing without the BBN relation.

Constraints on cosmological parameters are summarized in Tables 1, 2 and 3, where we fixed Y_p to 0.25, assumed the BBN relation and varied Y_p as a free parameter, respectively. In these tables, we present constraints only for the fiducial $\xi = 0.05$, as we found that dependencies of errors on the fiducial ξ is not significant except for σ_ξ ; as long as one

| | $\Omega_m h^2$ | $\Omega_b h^2$ | Ω_Λ | n_s |
|--------------|-----------------------|-----------------------|-----------------------|-----------------------|
| Planck | 2.86×10^{-3} | 1.95×10^{-4} | 2.01×10^{-2} | 6.06×10^{-3} |
| + SKA phase1 | 3.40×10^{-4} | 7.63×10^{-5} | 2.33×10^{-3} | 2.03×10^{-3} |
| + SKA phase2 | 2.52×10^{-4} | 7.40×10^{-5} | 9.26×10^{-4} | 1.42×10^{-3} |
| + Omniscope | 8.16×10^{-5} | 2.42×10^{-5} | 4.18×10^{-4} | 4.81×10^{-4} |
| CMBPol | 1.16×10^{-3} | 3.78×10^{-5} | 7.48×10^{-3} | 1.75×10^{-3} |
| + SKA phase1 | 3.11×10^{-4} | 2.91×10^{-5} | 2.14×10^{-3} | 1.20×10^{-3} |
| + SKA phase2 | 2.12×10^{-4} | 2.74×10^{-5} | 9.06×10^{-4} | 9.16×10^{-4} |
| + Omniscope | 5.13×10^{-5} | 1.31×10^{-5} | 4.09×10^{-4} | 3.68×10^{-4} |
| | $A_s \times 10^{10}$ | τ_{reion} | Σm_ν | ξ |
| Planck | 2.31×10^{-1} | 4.58×10^{-3} | 1.23×10^{-1} | 9.99×10^{-1} |
| + SKA phase1 | 1.88×10^{-1} | 4.36×10^{-3} | 3.69×10^{-2} | 1.58×10^{-1} |
| + SKA phase2 | 1.87×10^{-1} | 4.28×10^{-3} | 2.86×10^{-2} | 1.45×10^{-1} |
| + Omniscope | 1.84×10^{-1} | 4.15×10^{-3} | 1.13×10^{-2} | 6.09×10^{-2} |
| CMBPol | 1.10×10^{-1} | 2.46×10^{-3} | 4.26×10^{-2} | 1.51×10^{-1} |
| + SKA phase1 | 1.01×10^{-1} | 2.41×10^{-3} | 1.56×10^{-2} | 8.15×10^{-2} |
| + SKA phase2 | 9.95×10^{-2} | 2.37×10^{-3} | 1.10×10^{-2} | 7.69×10^{-2} |
| + Omniscope | 7.81×10^{-2} | 1.78×10^{-3} | 7.15×10^{-3} | 3.19×10^{-2} |

Table 1: 1σ errors on cosmological parameters for fiducial $\xi = 0.05$ for the cases with fixed $Y_p = 0.25$.

considers a fiducial $\xi \leq 0.1$, errors of cosmological parameters differ by no more than 25%. The only exception is σ_ξ which has been shown to depend on fiducial ξ in the absence of the BBN relation. Table 4 summarizes the dependence of σ_ξ on fiducial values of ξ . Except for the cases with the BBN relation, we see that σ_ξ scales almost proportionally to the inverse of fiducial ξ .

3.2 Cases with extra radiation

So far we have been investigating constraints on ξ in combination with CMB and 21 cm observations. Having observed that the combination of observations can improve constraints on ξ from only CMB ones, we extend our analysis to consider cosmological models with not only nonzero ξ but also extra (dark) radiation other than active neutrinos. Throughout this subsection, we assume that the extra radiation is massless. In addition, we assume the BBN relation $Y_p(\Omega_b h^2, \xi, \Delta N_\nu)$, which allows us to distinguish ξ and ΔN_ν even if the active neutrinos are almost massless.

In Fig. 3, we plot 2σ constraints in the ξ - ΔN_ν plane from CMB alone as well as combinations of CMB and 21 cm. Three different fiducial models $(\xi, \Delta N_\nu) = (0, 0.2)$,

| | $\Omega_m h^2$ | $\Omega_b h^2$ | Ω_Λ | n_s |
|--------------|-----------------------|-----------------------|-----------------------|-----------------------|
| Planck | 2.41×10^{-3} | 2.13×10^{-4} | 2.09×10^{-2} | 7.06×10^{-3} |
| + SKA phase1 | 3.04×10^{-4} | 9.35×10^{-5} | 2.30×10^{-3} | 2.22×10^{-3} |
| + SKA phase2 | 2.02×10^{-4} | 8.64×10^{-5} | 9.21×10^{-4} | 1.44×10^{-3} |
| + Omniscope | 7.94×10^{-5} | 1.54×10^{-5} | 4.15×10^{-4} | 3.54×10^{-4} |
| CMBPol | 9.27×10^{-4} | 4.83×10^{-5} | 7.16×10^{-3} | 2.54×10^{-3} |
| + SKA phase1 | 2.75×10^{-4} | 4.16×10^{-5} | 2.11×10^{-3} | 1.46×10^{-3} |
| + SKA phase2 | 1.43×10^{-4} | 4.05×10^{-5} | 9.00×10^{-4} | 1.04×10^{-3} |
| + Omniscope | 4.81×10^{-5} | 1.24×10^{-5} | 4.08×10^{-4} | 3.17×10^{-4} |
| | $A_s \times 10^{10}$ | τ_{reion} | Σm_ν | ξ |
| Planck | 2.07×10^{-1} | 4.64×10^{-3} | 1.28×10^{-1} | 4.50×10^{-2} |
| + SKA phase1 | 1.92×10^{-1} | 4.31×10^{-3} | 3.34×10^{-2} | 2.10×10^{-2} |
| + SKA phase2 | 1.89×10^{-1} | 4.25×10^{-3} | 2.45×10^{-2} | 1.83×10^{-2} |
| + Omniscope | 1.85×10^{-1} | 4.14×10^{-3} | 8.08×10^{-3} | 1.28×10^{-2} |
| CMBPol | 1.07×10^{-1} | 2.48×10^{-3} | 3.92×10^{-2} | 1.03×10^{-2} |
| + SKA phase1 | 1.01×10^{-1} | 2.39×10^{-3} | 1.55×10^{-2} | 7.85×10^{-3} |
| + SKA phase2 | 9.78×10^{-2} | 2.33×10^{-3} | 1.07×10^{-2} | 6.95×10^{-3} |
| + Omniscope | 6.86×10^{-2} | 1.56×10^{-3} | 5.30×10^{-3} | 4.04×10^{-3} |

Table 2: Same as in Table 1 but for the cases with the BBN relation.

| | $\Omega_m h^2$ | $\Omega_b h^2$ | Ω_Λ | n_s | |
|--------------|-----------------------|-----------------------|-----------------------|-----------------------|-----------------------|
| Planck | 3.31×10^{-3} | 2.27×10^{-4} | 2.11×10^{-2} | 7.56×10^{-3} | |
| + SKA phase1 | 3.46×10^{-4} | 1.09×10^{-4} | 2.34×10^{-3} | 2.25×10^{-3} | |
| + SKA phase2 | 2.66×10^{-4} | 1.05×10^{-4} | 9.26×10^{-4} | 1.46×10^{-3} | |
| + Omniscope | 8.31×10^{-5} | 3.88×10^{-5} | 4.18×10^{-4} | 4.87×10^{-4} | |
| CMBPol | 1.29×10^{-3} | 4.90×10^{-5} | 8.03×10^{-3} | 2.72×10^{-3} | |
| + SKA phase1 | 3.17×10^{-4} | 4.29×10^{-5} | 2.14×10^{-3} | 1.49×10^{-3} | |
| + SKA phase2 | 2.23×10^{-4} | 4.20×10^{-5} | 9.06×10^{-4} | 1.05×10^{-3} | |
| + Omniscope | 5.27×10^{-5} | 2.28×10^{-5} | 4.10×10^{-4} | 3.69×10^{-4} | |
| | $A_s \times 10^{10}$ | τ_{reion} | Σm_ν | ξ | Y_p |
| Planck | 2.32×10^{-1} | 4.66×10^{-3} | 1.28×10^{-1} | 1.12 | 1.13×10^{-2} |
| + SKA phase1 | 1.92×10^{-1} | 4.36×10^{-3} | 3.70×10^{-2} | 2.10×10^{-1} | 5.90×10^{-3} |
| + SKA phase2 | 1.89×10^{-1} | 4.29×10^{-3} | 2.88×10^{-2} | 2.05×10^{-1} | 5.41×10^{-3} |
| + Omniscope | 1.85×10^{-1} | 4.17×10^{-3} | 1.16×10^{-2} | 8.99×10^{-2} | 3.83×10^{-3} |
| CMBPol | 1.10×10^{-1} | 2.49×10^{-3} | 4.47×10^{-2} | 1.85×10^{-1} | 2.83×10^{-3} |
| + SKA phase1 | 1.02×10^{-1} | 2.42×10^{-3} | 1.57×10^{-2} | 1.01×10^{-1} | 2.15×10^{-3} |
| + SKA phase2 | 1.00×10^{-1} | 2.37×10^{-3} | 1.11×10^{-2} | 9.89×10^{-2} | 1.96×10^{-3} |
| + Omniscope | 7.94×10^{-2} | 1.91×10^{-3} | 7.47×10^{-3} | 4.93×10^{-2} | 1.31×10^{-3} |

Table 3: Same as in Table 1 but for the cases with freely varying Y_p .

- Fixing $Y_p = 0.25$

| | $\xi = -0.1$ | $\xi = 0.05$ | $\xi = 0.01$ |
|--------------|-----------------------|-----------------------|-----------------------|
| Planck | 5.01×10^{-1} | 9.99×10^{-1} | 4.88 |
| + SKA phase1 | 7.85×10^{-2} | 1.58×10^{-1} | 7.73×10^{-1} |
| + SKA phase1 | 7.23×10^{-2} | 1.45×10^{-1} | 6.76×10^{-1} |
| + Omniscope | 3.02×10^{-2} | 6.09×10^{-2} | 2.62×10^{-1} |
| CMBPol | 7.55×10^{-2} | 1.51×10^{-1} | 7.50×10^{-1} |
| + SKA phase1 | 4.07×10^{-2} | 8.15×10^{-2} | 4.05×10^{-1} |
| + SKA phase2 | 3.84×10^{-2} | 7.69×10^{-2} | 3.76×10^{-1} |
| + Omniscope | 1.59×10^{-2} | 3.19×10^{-2} | 1.52×10^{-1} |

- With the BBN relation

| | $\xi = -0.1$ | $\xi = 0.05$ | $\xi = 0.01$ |
|--------------|-----------------------|-----------------------|-----------------------|
| Planck | 3.72×10^{-2} | 4.50×10^{-2} | 4.29×10^{-2} |
| + SKA phase1 | 1.49×10^{-2} | 2.10×10^{-2} | 1.90×10^{-2} |
| + SKA phase2 | 1.29×10^{-2} | 1.83×10^{-2} | 1.65×10^{-2} |
| + Omniscope | 7.66×10^{-3} | 1.28×10^{-2} | 1.10×10^{-2} |
| CMBPol | 7.82×10^{-3} | 1.03×10^{-2} | 9.68×10^{-3} |
| + SKA phase1 | 5.89×10^{-3} | 7.85×10^{-3} | 7.31×10^{-3} |
| + SKA phase2 | 5.25×10^{-3} | 6.95×10^{-3} | 6.47×10^{-3} |
| + Omniscope | 2.86×10^{-3} | 4.04×10^{-3} | 3.65×10^{-3} |

- Freely varying Y_p

| | $\xi = -0.1$ | $\xi = 0.05$ | $\xi = 0.01$ |
|--------------|-----------------------|-----------------------|-----------------------|
| Planck | 5.61×10^{-1} | 1.12 | 5.42 |
| + SKA phase1 | 1.05×10^{-1} | 2.10×10^{-1} | 1.02 |
| + SKA phase2 | 1.02×10^{-1} | 2.05×10^{-1} | 9.06×10^{-1} |
| + Omniscope | 4.48×10^{-2} | 8.99×10^{-2} | 3.39×10^{-1} |
| CMBPol | 9.24×10^{-2} | 1.85×10^{-1} | 9.17×10^{-1} |
| + SKA phase1 | 5.07×10^{-2} | 1.01×10^{-1} | 5.03×10^{-1} |
| + SKA phase2 | 4.95×10^{-2} | 9.89×10^{-2} | 4.79×10^{-1} |
| + Omniscope | 2.46×10^{-2} | 4.93×10^{-2} | 2.24×10^{-1} |

Table 4: Dependence of σ_ξ on the fiducial value of ξ .

(0, 0.02) and $(-0.12, 0)$ are adopted here. We note that the latter two fiducial models give the similar effective numbers of neutrino species when neutrinos are relativistic. We can see that CMB alone cannot constrain ΔN_ν tightly. Moreover, the sizes of 2σ contours in the ΔN_ν direction are dependent on fiducial parameters ξ and ΔN_ν . This dependency should be suggesting that observations are not enough constraining and the likelihood surface in the ξ - ΔN_ν plane deviates from Gaussian cases to some extent. This may lead that when one explores constraints in a full parameter space using the Markov chain Monte Carlo, e.g., CosmoMC [31], resulting constraints would be somewhat less stringent than forecasts based on the Fisher matrix analysis. However, once we combine 21 cm observations, the constraints on ΔN_ν greatly improve. Moreover, the size of errors become almost independent of the fiducial values of ξ and ΔN_ν by an order of magnitude. This shows that combinations of CMB and 21 cm line observations will be promising to disentangle degenerating ξ and ΔN_ν . In Table 5, we present the 1σ constraints only for ξ and ΔN_ν . We note that regarding the constraints on other cosmological parameters, the inclusion of ΔN_ν does not degrade most of them significantly, or, by at most 50 %. Only exceptions are the constants on $\Omega_m h^2$ from Planck alone and $\Omega_b h^2$ from Planck+Omniscope and CMBPol+Omniscope, which are degraded by 2-3 times.

4 Summary

We have conducted a forecast for constraints on the lepton asymmetry ξ from the future 21 cm observations. A detection of a finite ξ from cosmological observations can give unique implications for the origin of the baryon asymmetry in our Universe. In our analysis, we have adopted the power spectra of the 21 cm signal from redshifts before the reionization, in combination with those of CMB. When we consider constraints on ξ in the absence extra radiation, we have found that, even without assuming the BBN relation, combinations of 21 cm and CMB observations can constrain ξ with a better accuracy than the primordial abundances of light elements, which cannot be achieved by CMB alone. On the other hand, once the BBN relation has been taken into account, even the sensitivity of CMB observations alone to ξ substantially improves, 21 cm observations however can still improve the constraints and be useful in constraining the lepton asymmetry. In addition, we have also investigated constraints on ξ in the presence of some extra radiation. We have shown that 21 cm observations can substantially improve the constraints on ΔN_ν from CMB alone, and allow us to distinguish between the lepton asymmetry and extra radiation. Our results should be indicating that 21 cm observations can be a powerful probe of neutrinos and the origin of matter in the Universe.

Acknowledgments

This work is partially supported by the Grant-in-Aid for Scientific research from the Ministry of Education, Science, Sports, and Culture, Japan, Nos. 21111006, 22244030,

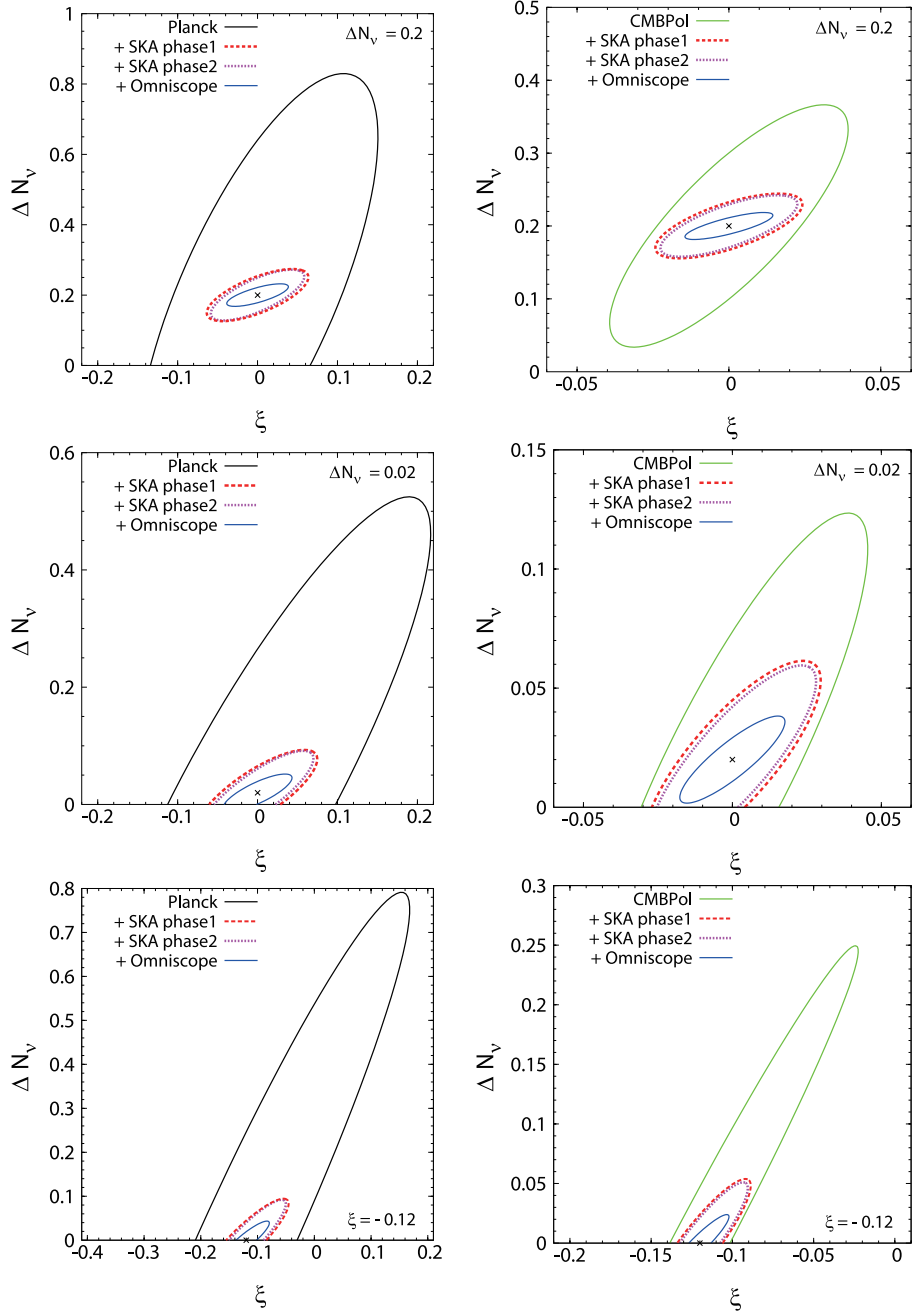


Figure 3: Expected 2σ constraints on the ξ - ΔN_ν plane. In this figure, the BBN relation is assumed. As fiducial values of $(\xi, \Delta N_\nu)$, we here adopt $(0.2, 0)$, $(0.02, 0)$ and $(0, -0.12)$ in the top, middle and bottom panels, respectively. Note that scales differ among different panels.

- fiducial $(\xi, \Delta N_\nu) = (0, 0.2)$

| | ξ | ΔN_ν |
|--------------|-----------------------|-----------------------|
| Planck | 6.07×10^{-2} | 2.54×10^{-1} |
| + SKA phase1 | 2.56×10^{-2} | 2.99×10^{-2} |
| + SKA phase2 | 2.36×10^{-2} | 2.91×10^{-2} |
| + Omniscope | 1.55×10^{-2} | 1.29×10^{-2} |
| CMBPol | 1.58×10^{-2} | 6.71×10^{-2} |
| + SKA phase1 | 9.77×10^{-3} | 1.79×10^{-2} |
| + SKA phase2 | 9.09×10^{-3} | 1.70×10^{-2} |
| + Omniscope | 5.83×10^{-3} | 7.47×10^{-3} |

- fiducial $(\xi, \Delta N_\nu) = (0, 0.02)$

| | ξ | ΔN_ν |
|--------------|-----------------------|-----------------------|
| Planck | 8.74×10^{-2} | 2.04×10^{-1} |
| + SKA phase1 | 3.01×10^{-2} | 2.94×10^{-2} |
| + SKA phase2 | 2.82×10^{-2} | 2.88×10^{-2} |
| + Omniscope | 1.74×10^{-2} | 1.28×10^{-2} |
| CMBPol | 1.83×10^{-2} | 4.17×10^{-2} |
| + SKA phase1 | 1.20×10^{-2} | 1.67×10^{-2} |
| + SKA phase2 | 1.13×10^{-2} | 1.59×10^{-2} |
| + Omniscope | 7.11×10^{-3} | 7.37×10^{-3} |

- fiducial $(\xi, \Delta N_\nu) = (-0.12, 0)$

| | ξ | ΔN_ν |
|--------------|-----------------------|-----------------------|
| Planck | 1.16×10^{-1} | 3.19×10^{-1} |
| + SKA phase1 | 3.02×10^{-2} | 3.81×10^{-2} |
| + SKA phase2 | 2.82×10^{-2} | 3.71×10^{-2} |
| + Omniscope | 1.64×10^{-2} | 1.75×10^{-2} |
| CMBPol | 3.93×10^{-2} | 1.01×10^{-1} |
| + SKA phase1 | 1.26×10^{-2} | 2.17×10^{-2} |
| + SKA phase2 | 1.19×10^{-2} | 2.06×10^{-2} |
| + Omniscope | 7.22×10^{-3} | 9.65×10^{-3} |

Table 5: 1σ errors on ξ and ΔN_ν for the case with the BBN relation and their dependence on fiducial $(\xi, \Delta N_\nu)$

23540327, 26105520 (K.K.), 23.5622 (T.S.), 25.4260 (Y.O.) and 23740195 (T.T.). K.K. is supported by the Center for the Promotion of Integrated Science (CPIS) of Sokendai (1HB5804100). T.S. is supported by the Academy of Finland grant 1263714.

Appendix

A Expressions for the coefficients C_i

Below we give explicit expressions for the coefficients C_i , which are necessary to obtain Eqs. (13) and (14).

$$C_0 = \frac{2}{e^y + 1}, \quad (24)$$

$$C_2 = \frac{e^y (e^y - 1)}{(e^y + 1)^3}, \quad (25)$$

$$C_4 = \frac{e^y (11e^y - 11e^{2y} + e^{3y} - 1)}{12 (e^y + 1)^5}, \quad (26)$$

$$C_6 = \frac{e^y (57e^y - 302e^{2y} + 302e^{3y} - 57e^{4y} + e^{5y} - 1)}{360 (e^y + 1)^7}, \quad (27)$$

$$C_8 = \frac{e^y (247e^y - 4293e^{2y} + 15619e^{3y} - 15619e^{4y} + 4293e^{5y} - 247e^{6y} + e^{7y} - 1)}{20160 (e^y + 1)^9}, \quad (28)$$

$$C_{10} = \frac{e^y (1013e^y - 47840e^{2y} + 455192e^{3y} - 1310354e^{4y} + 1310354e^{5y} - 455192e^{6y})}{1814400 (e^y + 1)^{11}} + \frac{e^y (47840e^{7y} - 1013e^{8y} + e^{9y} - 1)}{1814400 (e^y + 1)^{11}}. \quad (29)$$

B Non-relativistic limit of $\rho_\nu + \rho_{\bar{\nu}}$ and $p_\nu + p_{\bar{\nu}}$ for any ξ

Below we show the exact solutions for the $\rho_\nu + \rho_{\bar{\nu}}$ and $p_\nu + p_{\bar{\nu}}$ for any ξ in non-relativistic limit by using polylogarithm $\text{Li}_s(z)$, which is one of special functions.

$$\begin{aligned} \rho_\nu + \rho_{\bar{\nu}} &\simeq \frac{T_\nu^4 a \tilde{m}}{2\pi^2} \int_0^\infty y^2 dy \left[1 + \frac{1}{2} \left(\frac{y}{a \tilde{m}} \right)^2 \right] \left(\frac{1}{e^{y+\xi} + 1} + \frac{1}{e^{y-\xi} + 1} \right) \\ &= \frac{T_\nu^4 a \tilde{m}}{2\pi^2} [-2\{\text{Li}_3(-e^{-\xi}) + \text{Li}_3(-e^\xi)\}] + \frac{T_\nu^4}{4\pi^2 a \tilde{m}} [-24\{\text{Li}_5(-e^{-\xi}) + \text{Li}_5(-e^\xi)\}], \end{aligned} \quad (30)$$

$$\begin{aligned} p_\nu + p_{\bar{\nu}} &\simeq \frac{T_\nu^4}{6\pi^2 a \tilde{m}} \int_0^\infty y^4 dy \left[1 - \frac{1}{2} \left(\frac{y}{a \tilde{m}} \right)^2 \right] \left(\frac{1}{e^{y+\xi} + 1} + \frac{1}{e^{y-\xi} + 1} \right) \\ &= \frac{T_\nu^4}{6\pi^2 a \tilde{m}} [-24\{\text{Li}_5(-e^{-\xi}) + \text{Li}_5(-e^\xi)\}] - \frac{T_\nu^4}{12\pi^2 (a \tilde{m})^3} [-720\{\text{Li}_7(-e^{-\xi}) + \text{Li}_7(-e^\xi)\}]. \end{aligned} \quad (31)$$

If we expand these formulas around $\xi = 0$, they reduce to Eqs. (13) and (14).

C BBN relation

In the early universe with a higher temperature than $O(1)$ MeV the inter-converting reactions between neutron and proton through the weak interaction ($n + e^+ \leftrightarrow p + \nu_e$, $n + \bar{\nu}_e \leftrightarrow p + e^-$, and $n \leftrightarrow p + e^- + \nu_e$) were sufficiently rapid. In this case the neutron to proton ratio obeys its thermal equilibrium value,

$$\frac{n}{p} = \exp \left[-\frac{\Delta m_{np} + \mu_{\nu_e}}{T} \right] = \exp \left[-\frac{\Delta m_{np}}{T} - \xi_{\nu_e} \right], \quad (32)$$

with the mass difference $\Delta m_{np} = 1.3$ MeV. Here we explicitly wrote the degeneracy parameter of ν_e to be $\xi_{\nu_e} = \mu_{\nu_e}/T_\nu$ with μ_{ν_e} being the chemical potential of ν_e . It is remarkable that the electron's chemical potential μ_{e^-} must be much smaller than that of ν_e because of the neutrality of the Universe $\xi_e = \mu_{e^-}/T \sim O(\eta) \ll \xi_{\nu_e}$ with T and η being the photon temperature and the baryon-to-photon ratio, respectively. Accordingly ξ_{ν_e} affects the freezeout value of n/p , which can change the light element abundances. In particular Y_p depends on ξ_{ν_e} in addition to η (or $\Omega_b h^2$) and N_ν . Thus Y_p is related to those three parameters i.e., $Y_p = Y_p(\Omega_b h^2, \xi_{\nu_e}, \Delta N_\nu)$, which is called "the BBN relation."

Since we need quite a precise value of Y_p in the current studies, we numerically compute Y_p as functions of those three parameters without adopting known fitting formula (e.g., given in Ref. [32]). In this computation, we have used the most recent data for nuclear reaction rates [33–37].

In Fig. 4, as a reference, we plotted allowed regions in the $\eta - \xi_{\nu_e}$ plane at the 68% and the 95% C.L, respectively. Here we set $\Delta N_\nu = 0$. We have adopted the following observational light element abundances, $Y_p = 0.2534 \pm 0.0083$ (68%) [38] and $D/H = n_D/n_H = (2.535 \pm 0.050) \times 10^{-5}$ (68%) [39].

References

- [1] K. Kohri, M. Kawasaki and K. Sato, *Astrophys. J.* **490**, 72 (1997) [astro-ph/9612237].
- [2] K. Sato, K. Kohri and M. Kawasaki, RESCEU-59-98.
- [3] L. A. Popa and A. Vasile, *JCAP* **0806**, 028 (2008) [arXiv:0804.2971 [astro-ph]].
- [4] M. Shiraishi, K. Ichikawa, K. Ichiki, N. Sugiyama and M. Yamaguchi, *JCAP* **0907**, 005 (2009) [arXiv:0904.4396 [astro-ph.CO]].
- [5] A. Caramete and L. A. Popa, arXiv:1311.3856 [astro-ph.CO].

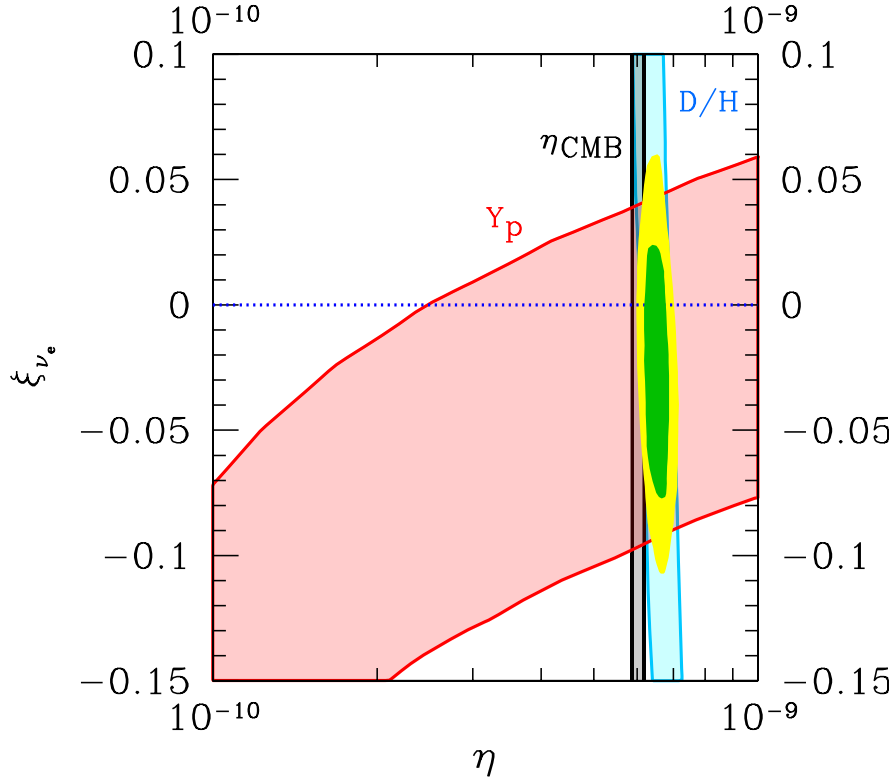


Figure 4: Regions allowed by the BBN alone in the $\eta - \xi_{\nu_e}$ plane. The 68% and the 95% C.L. contours are plotted, respectively. Here we set $\Delta N_\nu = 0$. The vertical band represents the baryon to photon ratio reported by Planck $\eta = (6.04 \pm 0.15) \times 10^{-10}$ at 95% C.L.. The line of each light element corresponds to the individual constraint at 95% C.L..

- [6] A. Casas, W. Y. Cheng and G. Gelmini, Nucl. Phys. B **538**, 297 (1999) [hep-ph/9709289].
- [7] J. March-Russell, H. Murayama and A. Riotto, JHEP **9911**, 015 (1999) [hep-ph/9908396].
- [8] J. McDonald, Phys. Rev. Lett. **84**, 4798 (2000) [hep-ph/9908300].
- [9] M. Kawasaki, F. Takahashi and M. Yamaguchi, Phys. Rev. D **66**, 043516 (2002) [hep-ph/0205101].
- [10] F. Takahashi and M. Yamaguchi, Phys. Rev. D **69**, 083506 (2004) [hep-ph/0308173].
- [11] D. J. Schwarz and M. Stuke, JCAP **0911**, 025 (2009) [Erratum-ibid. **1010**, E01 (2010)] [arXiv:0906.3434 [hep-ph]].
- [12] V. B. Semikoz, D. D. Sokoloff and J. W. F. Valle, Phys. Rev. D **80**, 083510 (2009) [arXiv:0905.3365 [hep-ph]].
- [13] C. Gordon and K. A. Malik, Phys. Rev. D **69**, 063508 (2004) [astro-ph/0311102].
- [14] D. H. Lyth, C. Ungarelli and D. Wands, Phys. Rev. D **67**, 023503 (2003) [astro-ph/0208055].
- [15] E. Di Valentino, M. Lattanzi, G. Mangano, A. Melchiorri and P. Serpico, Phys. Rev. D **85**, 043511 (2012) [arXiv:1111.3810 [astro-ph.CO]].
- [16] <http://www.skatelescope.org>
- [17] M. Tegmark and M. Zaldarriaga, Phys. Rev. D **82**, 103501 (2010) [arXiv:0909.0001 [astro-ph.CO]].
- [18] J. Tauber *et al.* [Planck Collaboration], astro-ph/0604069.
- [19] D. Baumann *et al.* [CMBPol Study Team Collaboration], AIP Conf. Proc. **1141**, 10 (2009) [arXiv:0811.3919 [astro-ph]].
- [20] C. -P. Ma and E. Bertschinger, Astrophys. J. **455**, 7 (1995) [astro-ph/9506072].
- [21] J. Lesgourgues and S. Pastor, Phys. Rev. D **60**, 103521 (1999) [hep-ph/9904411].
- [22] A. Lewis, A. Challinor and A. Lasenby, Astrophys. J. **538**, 473 (2000) [astro-ph/9911177].
- [23] S. Furlanetto, S. P. Oh and F. Briggs, Phys. Rept. **433**, 181 (2006) [astro-ph/0608032].

- [24] J. R. Pritchard and A. Loeb, Rept. Prog. Phys. **75**, 086901 (2012) [arXiv:1109.6012 [astro-ph.CO]].
- [25] M. McQuinn, O. Zahn, M. Zaldarriaga, L. Hernquist and S. R. Furlanetto, Astrophys. J. **653**, 815 (2006) [astro-ph/0512263].
- [26] Y. Oyama, A. Shimizu and K. Kohri, Phys. Lett. B **718**, 1186 (2013) [arXiv:1205.5223 [astro-ph.CO]].
- [27] K. Kohri, Y. Oyama, T. Sekiguchi and T. Takahashi, JCAP **1310**, 065 (2013) [arXiv:1303.1688 [astro-ph.CO]].
- [28] A. D. Dolgov, S. H. Hansen, S. Pastor, S. T. Petcov, G. G. Raffelt and D. V. Semikoz, Nucl. Phys. B **632**, 363 (2002) [hep-ph/0201287].
- [29] P. A. R. Ade *et al.* [Planck Collaboration], arXiv:1303.5076 [astro-ph.CO].
- [30] G. Steigman, Adv. High Energy Phys. **2012**, 268321 (2012) [arXiv:1208.0032 [hep-ph]].
- [31] A. Lewis and S. Bridle, Phys. Rev. D **66**, 103511 (2002) [astro-ph/0205436].
- [32] G. Steigman, Ann. Rev. Nucl. Part. Sci. **57**, 463 (2007) [arXiv:0712.1100 [astro-ph]].
- [33] M. S. Smith, L. H. Kawano and R. A. Malaney, Astrophys. J. Suppl. **85**, 219 (1993).
- [34] C. Angulo *et al.*, Nucl. Phys. A **656**, 3 (1999).
- [35] R. H. Cyburt, B. D. Fields and K. A. Olive, New Astron. **6**, 215 (2001); R. H. Cyburt, Phys. Rev. D **70**, 023505 (2004).
- [36] P. D. Serpico, S. Esposito, F. Iocco, G. Mangano, G. Miele and O. Pisanti, JCAP **0412**, 010 (2004).
- [37] R. H. Cyburt and B. Davids, arXiv:0809.3240 [nucl-ex].
- [38] E. Aver, K. A. Olive and E. D. Skillman, JCAP **1204**, 004 (2012) [arXiv:1112.3713 [astro-ph.CO]].
- [39] M. Pettini and R. Cooke, Mon. Not. Roy. Astron. Soc. **425**, 2477 (2012) [arXiv:1205.3785 [astro-ph.CO]].